CONTINUOUS AND DISCRETE WAVELET TRANSFORMS BASED ANALYSIS OF WEATHER DATA OF NORTH WESTERN REGION OF SAUDI ARABIA

**Mohamed A. El-Gebeily[1], Shafiqur Rehman[2] ,
Luai M. Al-Hadhrami[2] and Jaafar AlMutawa[1]**

King Fahd University of Petroleum and Minerals, Saudi Arabia

Abstract: The present study utilizes daily mean time series of meteorological parameters (air temperature, relative humidity, barometric pressure and wind speed) and daily totals of rainfall data to understand the changes in these parameters during 17 years period i.e. 1990 to 2006. The analysis of the above data is made using continuous and discrete wavelet transforms because it provides a time–frequency representation of an analyzed signal in the time domain. Moreover, in the recent years, wavelet methods have become useful and powerful tools for analysis of the variations, periodicities, trends in time series in general and meteorological parameters in particular. In present study, both continues and discrete wavelet transforms were used and found to be capable of showing the increasing or decreasing trends of the meterorological parameters with. The seasonal variability was also very well represented by the wavelet analysis used in this study. High levels of compressions were obtained retaining the originality of the signals.

Keywords: *weather; meteorology; compression, decomposition, wavelet transform, trend analysis*

INTRODUCTION

Climate change on global, regional, and local scales is of great concern and has been the focus of attention of many researchers in the fields of science, engineering and social studies throughout the world. This is because the long-term climate variability is of great importance for the estimation of its impact on human activities and for predicting future behavior. Over the past century or so the world has warmed by approximately 0.6°C, as quoted by Nicholas and Collins (2006). According to IPCC report (2001) and Meehl et al, (2004), there is strong evidence that most of the global warming over the past 50 years is likely to have been due to increases in greenhouse gas concentrations. The climatic studies are very common

[1] Department of Mathematics and Statistics, King Fahd University of Petroleum and Minerals, Dhahran-31261, Saudi Arabia, E-mail: mgebeily@kfupm.edu.sa, jaafarm@kfupm.edu.sa, Homepage: http://faculty.kfupm.edu.sa/ math/mgebeily   http://faculty.kfupm.edu.sa/math/jaafarm
[2] Center for Engineering Research, Research Institute, King Fahd University of Petroleum and Minerals, Dhahran-31261, Saudi Arabia, E-mail: srehman@kfupm.edu.sa Homepage: http://faculty.kfupm.edu.sa/ri/srehman

and have been conducted in almost every part of the world, for example Freiwana and Kadioglub (2008) for Jordan, Elagib and Addin Abdu (1997) for Bahrain and Alkolibi (2002) for Saudi Arabia.

The wavelet transform is a strong mathematical tool that provides a time–frequency representation of an analyzed signal in the time domain as reported by Dabuechies (1990) and Percival and Walden (2000). Currently, wavelet methods are being used as powerful tools for the analysis of variations, periodicities, trends in time series (Partal and Kucuk, 2006; Pisoft et. al., 2004; and Yueqing et al., 2004).

Wavelet transforms have been used to investigate trends in the central England temperature series (Baliunas *et al.*, 1997); to study hemispheric temperature series and the southern oscillation index (Sonechkin *et al.*, 1999); to detect shifts in global temperature (Park and Mann, 2000); and to analyze variability in European temperatures (Datsenko *et al.*, 2001). Ding et. al. (2002) used wavelet transform to understand the frequency features of the Hong Kong temperature data. The climate parameters were analyzed by Lau and Weng (1995) using wavelet methods to detect and highlight the climatic features of the signal.

In this work we use continuous and discrete wavelet transforms to analyze the meteorological records (temperature, barometric pressure, precipitation, wind speed and relative humidity) of the weather station at Arar in the north western part of Saudi Arabia over the 17 year period from 1990 to 2006. Our goals are to identify the long term trends, detect periodicity and anomalous events and to study the compression of the records. It will be seen that wavelet tools provide clear indications of the sought events as well as a powerful tool for data compression.

SITE AND DATA DESCRIPTION

Arar is a town located in the north western part of Saudi Arabia. The latitude, longitude and the altitude of the data collection station are 30°54', 41°08' and 542 meters, respectively. The population of this region has increased during last couple of decades and economical growth has taken place. As a result of which the number cars on the road, air transport in the region, the infrastructure, the support services, etc. have increased exponentially. So, to understand the local effect on weather parameters of the region, daily mean values of air temperature, relative humidity, barometric pressure, wind speed and daily totals of rainfall data are used during the period of 1990 to 2006. This data is collected and managed by the Presidency of Meteorology and Environment (PME) at the national airport in Arar.

The air temperature at Arar was found to vary between a minimum of -0.7°C and 40.4°C while the overall mean remained as 22.2°C. In this region, higher air temperatures of >25°C were observed during the months of May to September during the year. The minimum temperatures were observed in the months of December and January. The barometric pressure varied between a minimum of 936mb and a maximum of 967mb while the overall mean remained as 949.6mb. The relative humidity was found to vary between a minimum of 17.7% and a maximum of 65%. The overall mean relative humidity in the region during entire data collection period was 36%. Higher values of relative humidity were observed during winter months (October to March) and lower during May to September. The wind speed was found to vary between 0 and 25 knots while the overall mean was found to be 7 knots. Higher wind speeds were observed in the months of January

at Arar varied between 0 and 38mm with an average of 0.13mm. Most of the rainfall occurs in the months of October to April and almost no rain during May to September.

A BACKGROUND ON WAVELETS

A signal or a time series such as the daily mean temperatures or the daily rainfall totals usually contains information of very different sizes: daily values, seasonal values, long-term values, abrupt events, etc. To analyze such behavior we need to use time-frequency atoms with varying support in time so as to be able to concentrate on the various features of the signal. Such time frequency atoms are called wavelets. A (real) wavelet $\psi(t)$ is a finite energy signal with zero average. A family of time-frequency atoms is obtained by the scaling and translation of $\psi(t)$:

$$\psi_{a,b}(t) = \frac{1}{\sqrt{a}} \psi\left(\frac{t-b}{a}\right).$$

Roughly speaking, the scale a corresponds to a frequency $\omega = 1/a$. Therefore a low scale corresponds to a high frequency, which translates into a compressed wavelet. This feature enables wavelets to identify the various frequency contents of the signal. The translation parameter b moves the wavelet in time. This means that wavelets are also capable of identifying the onset of a particular varied frequency event in time. To clarify the similarity and dissimilarity with the Fourier transform, consider the Fourier series of a typical time series such as a meteorological record or, more generally, a signal f:

$$f(t) = \sum a_n \sin nt + b_n \cos nt.$$

The rough meaning of this representation is that we think of f as (an infinite) superposition of harmonics with frequencies $n = 1,2,\dots$. The coefficients a_n, b_n tell us how much of the signal's energy is allocated at frequency n. What these coefficients are incapable of doing is provide information about their change in time. Thus if the signal goes through an abrupt change at a specific time instant the event is not indicated by the Fourier coefficients. By contrast, the wavelet series of f takes the form

$$f(t) = \sum_{m,n} C_{mn} \psi_{mn}(t),$$

where $\psi_{mn}(t) = \psi_{a_m \cdot b_n}(t)$ and where a_m, b_n are particularly chosen scale and time instances (see below). Here the coefficients C_{mn} represent the energy content of the signal at the scales a_m and times b_n, $m,n = \dots,-1,0,1,\dots$. It is then immediately clear that we have a fuller description of the signal; one which captures the scale as well as the time events. In this respect, low scale values a_m correspond to rapidly progressing components of the signal while high scale values correspond to slowly evolving components or low-frequency components. Since the coefficient C_{mn} depends also on the time instant b_n we are able to track the time history of the coefficient by fixing the value of m and changing the value of n. This ability to tap information about time events is extremely important in meteorological studies and this point will become vividly clear throughout this paper.

We use two types of wavelet transforms, namely the continuous wavelet transform and the discrete wavelet transform. The continuous wavelet transforms (CWT), in which the energy coefficients are computed for every possible scale a and time b rather than a sequence (a_m,b_n) of them. For this

type the energy coefficients of a signal f are given by

$$C(a,b) = \int_{-\infty}^{\infty} f(t) \psi_{a,b}(t) dt.$$

Here the coefficient $C(a,b)$ is a function of the two continuous variables a and b. The graphical representation of these coefficients requires 3D techniques. One can either use 3D graphics or an equivalent 2D method such as contours or colored schemes. In this paper, we use the commercially available Wavelet Toolbox in the software MATLAB® which uses colored schemes. To illustrate the use of this colored scheme we refer to Figure 2 below which shows a typical transform of a temperature time series. The top pane in that figure plots the temperature time series (or the signal) where the horizontal axis represents the number of days since January first, 1990 and the vertical axis represents the temperature. The middle pane shows the coefficients $C(a,b)$, which is where the color scheme is used. Here the horizontal axis represents the time b and the vertical axis represents the scale a and the color at the point (a,b) represents the value of the coefficient $C(a,b)$ with lighter colors representing higher values and darker colors representing lower values as depicted in the color key below the pane. The bottom pane in Figure 2 represents a cross section of the "3D colored picture" of the middle pane made by fixing the scale at $a = 1$ and changing the time b. Thus, the horizontal axis represents time whiles the vertical axis represents the actual value of $C(1,b)$ that is the value which appeared in color in the middle pane. This is called a coefficient line. The wavelet toolbox provides the capability of choosing a scale level; say $a = 20$; $a = 300$ and so on, to draw the coefficient line which would correspond to the chosen cross section of the colored picture.

It turns out that computing the coefficients $C(a,b)$ at all possible scales and times is not necessary to recover all information about the signal. We can perfectly recover the whole signal f from the coefficients calculated at the so called dyadic scale-space grid of points $(a_m, b_n) = (2^m, n2^m)$, $m, n = ..., -1, 0, 1, ...$. The coefficients $C_{mn} := C(a_m, b_n)$ computed this way constitute what we call the discrete wavelet transform (DWT) of the signal f. One important feature of the dyadic points to be observed here is that the time values $b_n = n2^m$ depend on the scale values $a_m = 2^m$. This means that small scales (progressively negative values of m) correspond to more closely located time instants b_n and vice versa. Therefore, at small scales, which correspond to the fast changing components of the signal changes, we take closely separated time instances to capture any fast evolving events while at large scales, which correspond to the slowly changing components of the signal, fewer time instants are necessary to capture the evolving events.

Hence, the DWT inherits all the important properties of the CWT in addition to being computationally fast. The DWT of a signal $f(t)$ which is represented by N values requires only $o(N)$ operations which is even faster than the fast Fourier transform (FFT) which takes $o(N \log N)$ operations. Add to that the ability of the DWT to analyze the signal in both frequency and time as compared to the frequency analysis only provided by the FFT.

In practice, all the wavelets corresponding to large scales (say, all scales larger than 2^M) are lumped up into one function $\varphi(t)$ called the scaling function (see Malat (1998)) which has all the properties of wavelets except that its average value is not zero. The complete decomposition of a signal f in this case takes the form

$$f(t) = \sum_n a_n \varphi_{M,n}(t) + \sum_{m<M,n} d_{m,n} \psi_{m,n}(t).$$

For each n in the above representation, the energy coefficient a_n can be thought of as providing weighted averages of the signal f over the span of the scaling function $\varphi_{M,n}(t)$, while the coefficients d_{mn} provide fluctuations (or details) around these averaged values at the various scales m. In the sequel we will be referring to this break down of the signal as approximation and details. When $\varphi_{M,n}(t)$ is slowly changing, a_n provides an approximation of the averaged values, or the trend, of the signal f itself. The flatter the function φ is the closer the values of the a_n's are to the trend in f. Such is the case, for example, with the scaling function corresponding to the Haar wavelet which is a completely flat function. Figure 7 and Figure 8 below show a temperature time series and its trend part at level $n = 11$ and a detail at level $m = 7$ using the Haar wavelet. The trend level 11 means, as discussed above, that all scales higher than 2^{11} days inclusive are lumped up in the scaling function. The detail level 7 means that the fluctuations at the scale 2^7 days are shown. Thus, events of duration around 128 days are captured at that level.

From a different viewpoint, the coefficients a_n and d_{mn} also provide a measure of the local similarity of the signal f to the scaling function $\varphi_{M,n}(t)$ and the wavelet $\psi_{mn}(t)$, respectively. Therefore, the degree of smoothness of $\varphi_{M,n}(t)$ tells us about the presence of a similarly smooth component of the signal or the lack thereof.

Analysis of a signal with wavelet packet transforms consists of breaking down each of the approximation and detail components of the signal at each level into "approximation and detail". The operation count in this process is back to $o(N \log N)$ but we gain more insight into the time-frequency behavior of the signal in terms of sharper isolation of fast events and the ability to come up with an optimal decomposition into constituent components (see, e.g., Walnut (2002)).

ANALYSIS OF AIR TEMPERATURE WITH THE CONTINUOUS WAVELET TRANSFORM (CWT)

The temperature data is recorded on an hourly basis and is stored as daily means at Arar meteorological data collection station located at the domestic airport. The temperature records are degrees Celsius versus days during the period from January 1st, 1990 to December 31st, 2006, a total of 6209 days. A very small number of data records had to be discarded due to measurement and/or recording errors. Since the wavelet toolbox of MATLAB® does not allow the flexibility of relabeling the axis, we have produced a conversion chart that should help see the correspondence between the year and the number of days since January 1, 1990. This is shown in Figure 1. Figure 2 shows the temperature data (top) from Arar (for a total of 6178 days), its continuous wavelet transform (or scalogram) (middle) and the wavelet coefficients at a scale $a \approx 1$ day (bottom). These coefficients are of the order of 10^{-15} which means that we merely see noise due to measurement errors (see the coefficient line at the bottom of the figure).

To see the daily temperature fluctuations we draw a coefficient line at a scale $a = 3$. This is shown in Figure 3. The coefficient line indicates that there are lesser fluctuations during the summer and the beginning of fall than the other seasons of the year. To see this, consider the part of the graph between day 1 and day 1000, a period of a little less than three years. During this period we see patterns of higher fluctuations followed
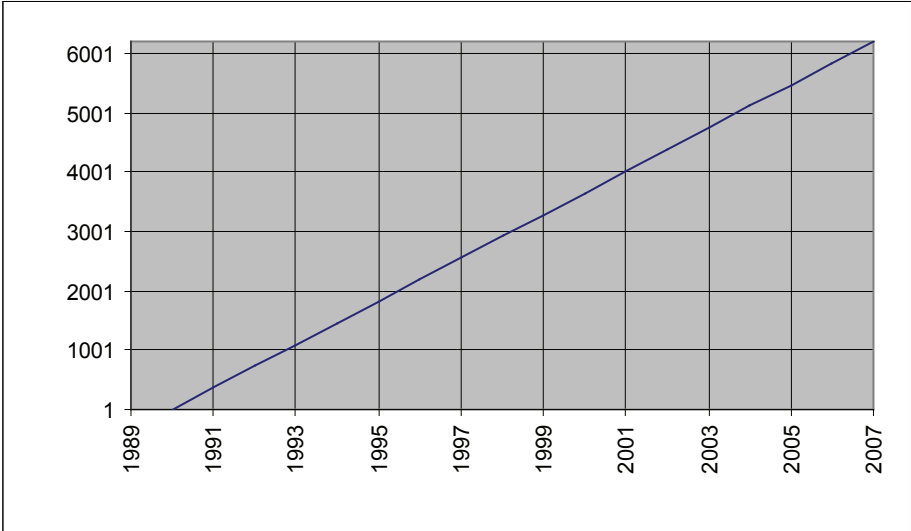
Figure 1   Correspondence between the year and the number of days since January 1, 1990

by lesser fluctuations. The first period of lesser fluctuations occurs at about 180 to 280 days from Jan 1. These are the summer months of June, July and August along with the fall month of September. This pattern of fluctuations repeats itself.

To see the monthly fluctuations we draw a coefficient line at a scale of the order of months. Figure 4 shows the coefficient line at the monthly level $a = 74$. This coefficient line is composed of slower sinusoidal fluctuations on top of which we can see faster fluctuation of relatively small magnitudes. In the jargon of Fourier series, these are higher harmonic fluctuations. These higher harmonics are also visible in the scalogram of the continuous wavelet transform as high amplitude; low duration waves on top of regular fluctuations (see Figure 2, for scales around 80). Finally, the smooth seasonal fluctuations (Figure 5) are obtained by drawing the coefficient line at the $a = 370$ days.

We would like to mention that long term trends (of scales of several years) such as

heating or cooling trends can also be detected from scalograms by increasing the maximum scale for the analysis (say, $a_{max} = 800$ instead of the value $a_{max} = 370$ depicted in Figure 2). However, these trends are more easlily detected from the discrete wavelet transform which we will consider next.

ANALYSIS WITH AIR TEMPERATURE USING DISCRETE WAVELET TRANSFORM (DWT)

To detect the long term trend of the temperature records at the Arar station we took the DWT of the time series with the Haar Wavelet and 11 levels of resolution. At this level of resolution, the span of each scaling wavelet is $2^{11} = 2048$ days and the whole length of the 17 year data record (1990-2006) is covered by $6209/2048 \approx 3$ wavelets. Figure 6 shows the signal and its approximation (trend) at 11 levels. Each wavelet produces an average value of the signal in its span, which explains the breaks we see in the graph of the approxi-
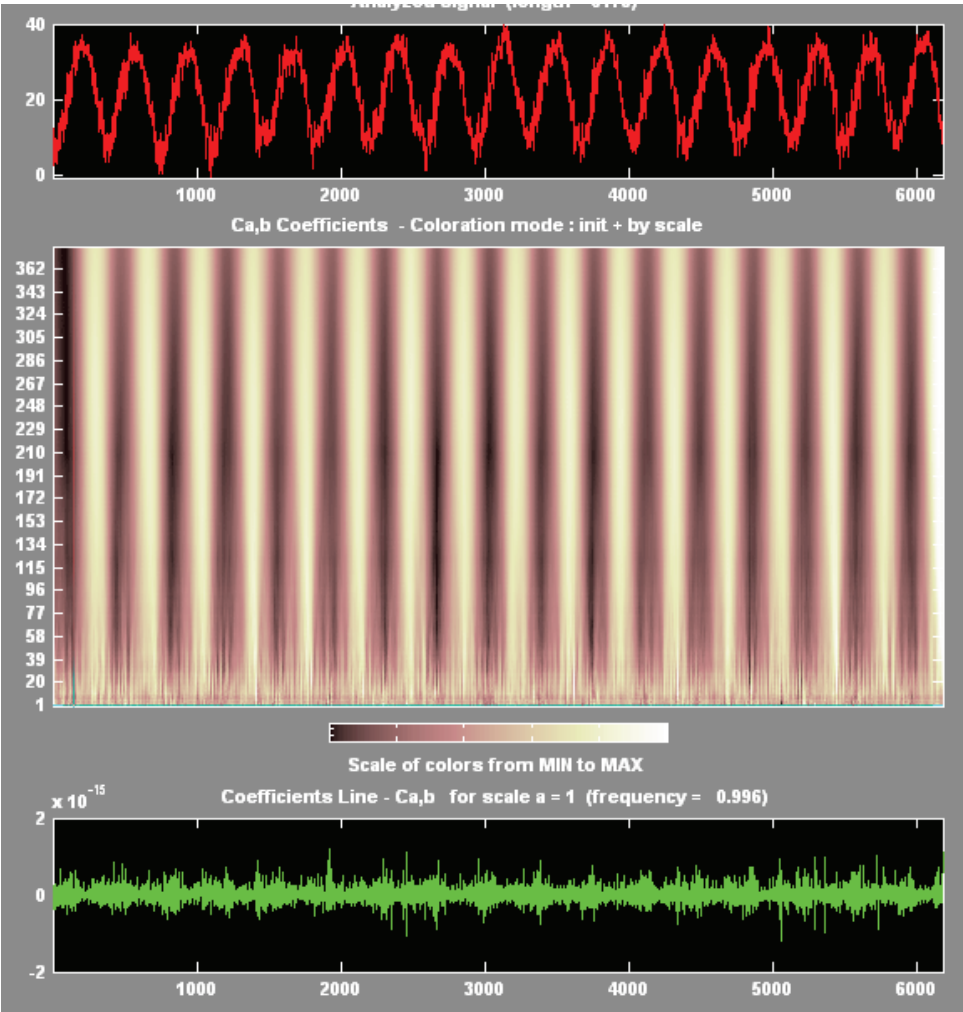
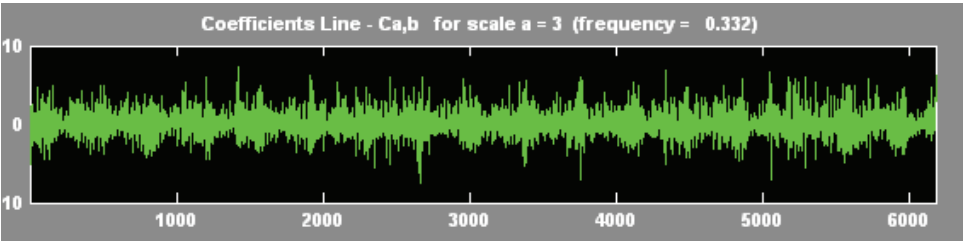**Figure 2** Temperature records of Arar and its continuous wavelet transform

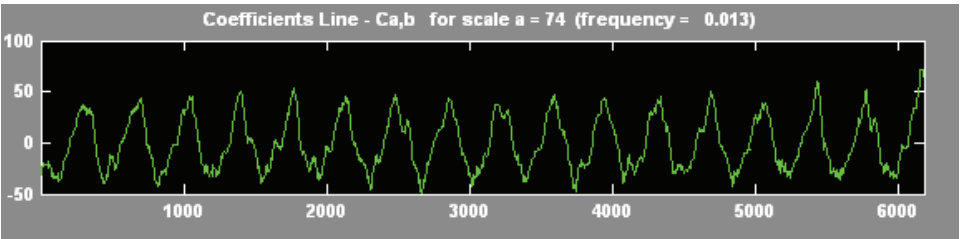**Figure 3** Wavelet coefficient line at scale a=3

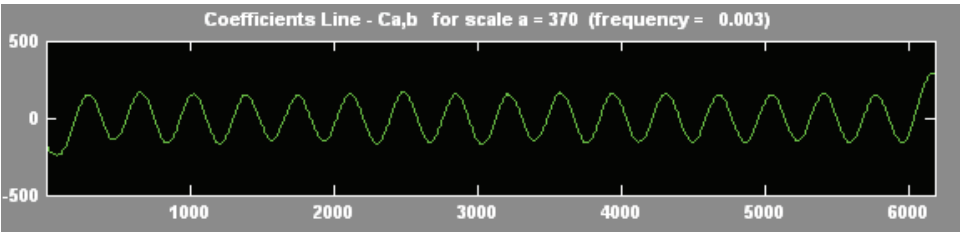**Figure 4** Wavelet coefficient line at scale a=74

Figure 5 Wavelet coefficient line at scale a=370

mation a_{11} in the figure. A general trend of heating (an increase in the mean temperature of about 2°C) is clear from the approximation signal a_{11}. A linear regression analysis of the same data was carried out in Rehman and El-Gebeily and it also confirmed the same trend. The higher harmonics fluctuations observed in the CWT (Figure 4) are still visible at the 7th detail level ($2^7 = 128$ days) of Figure 7.

The DWT of the temperature time series from Arar using the Meyer wavelet is shown in Figure 8. The Meyer wavelet has two features that make them very useful in analyzing temperature records: first, they are fairly smooth and second, they have limited frequency bands. The smoothness feature makes them more capable of detecting the smooth component of the signal as discussed earlier. The finite frequency bandwidth enables them to detect and isolate the various periodic components of the record. As a result, we can tell that the smooth component of the temperature signal (a_8 of Figure 8) went through a sharp
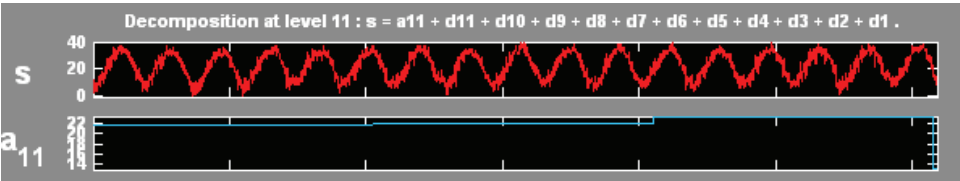

Figure 6 DWT of Arar temperature records with the Haar wavelet

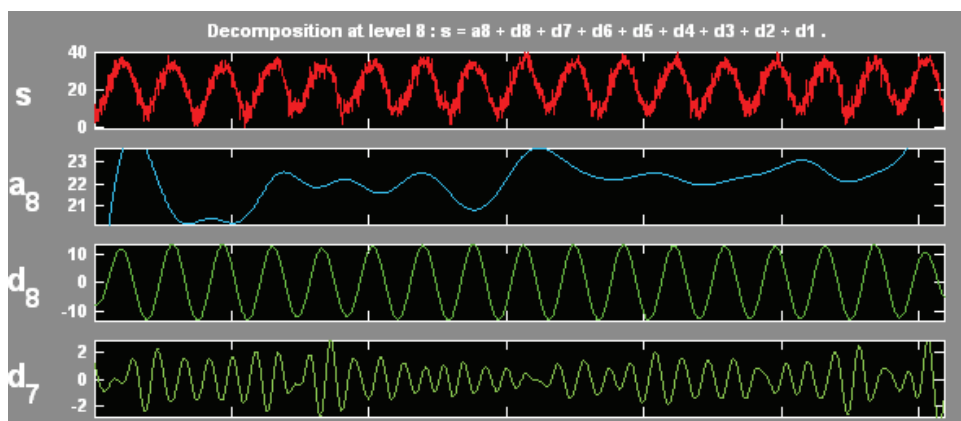**Figure 7** Seasonal fluctuations with higher harmonics

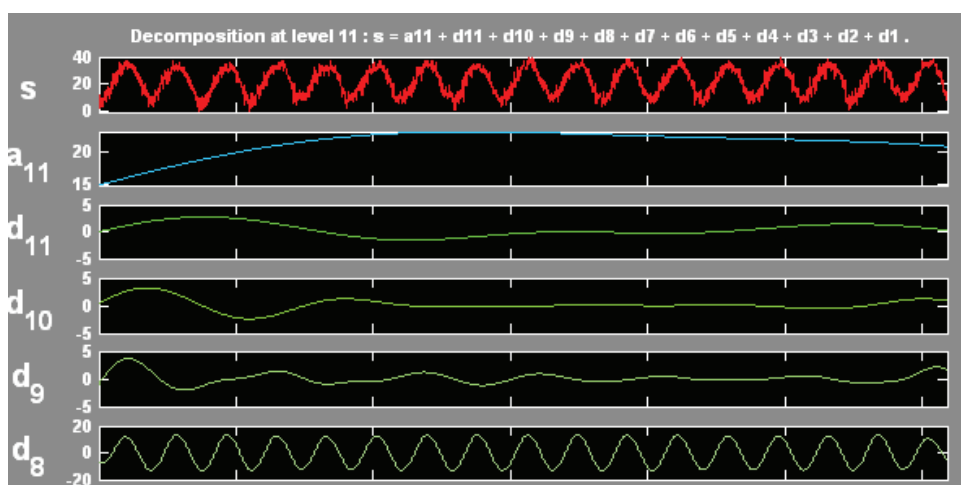**Figure 8** DWT of Arar temperature records with the Meyer wavelet

Figure 9 Detailed analysis of the trend line of Figure 8.

change during the year 1991 at the time of the gulf war. In addition to this we still see that the heating trend as the graph tends to keep rising over the years. We also see the periodic seasonal changes in the detail d_8 ($2^8 = 256$ days, 8.5 months, or two seasons). As before, higher harmonic components are visible at the detail level d_7. More details about the trend line a8 can be obtained by increasing the level of analysis to, say 11, instead of 8. The result is shown in Figure 9. In this case $a_8 = a_{11} + d_{11} + d_{10} + d_9$. We still get the sharp change around 1991

as the sum of the corresponding values from a_{11}, d_{11}, d_{10} and d_9.

ANALYSIS OF AIR TEMPERATURE WITH WAVELET PACKETS (WP)

Wavelet packets are more efficient than ordinary wavelets in that they are more capable of pinpointing the distribution of the energy coefficients for each scale. Figure 10 shows the wavelet packet analysis of the Arar temperature record. The analysis was made
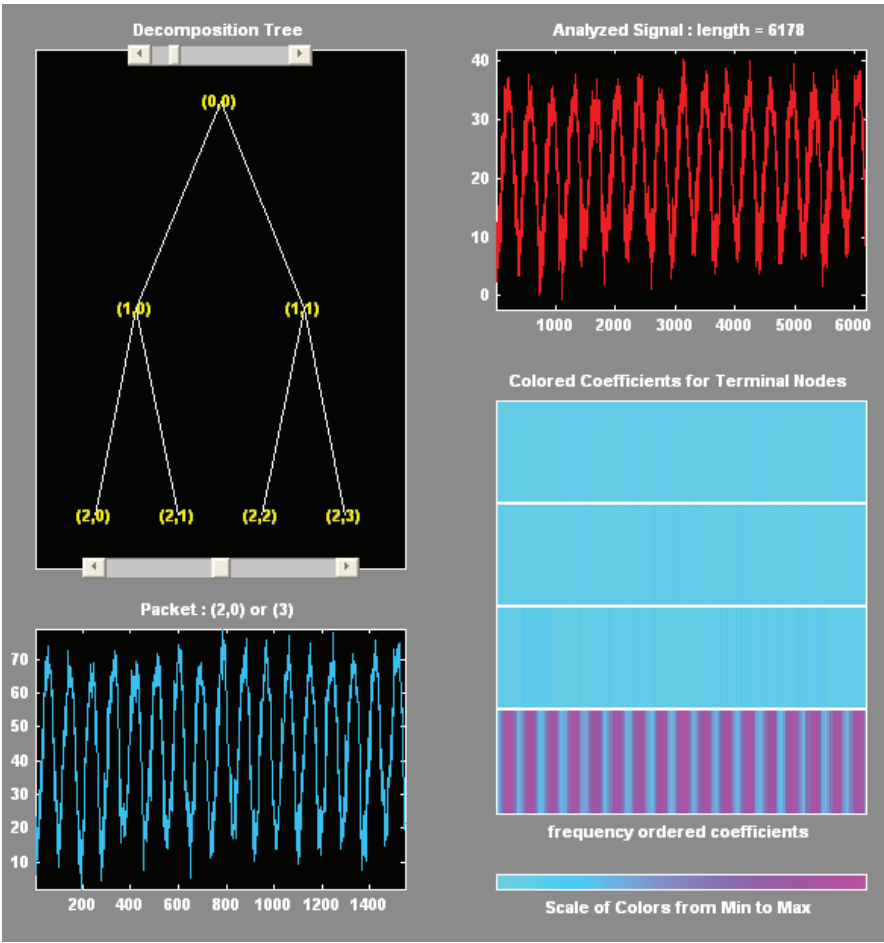
Figure 10 The DB3 WP analysis of the Arar temperature records

here using the Daubichi wavelet packet db3 with depth of analysis 2. Referring to Figure 10, the tree diagram displays the various components of the analyzed signal. Node (0,0) corresponds to the original signal. At the first level of analysis the original signal is analyzed into two components an approximation, which corresponds to node (1,0) and a detail component which corresponds to node (1,1). At the second level of analysis, both approximation signal (1,0) and the detail signal are again decomposed into approximation and detail. We thus obtain the nodes (2,0), (2,1), (2,2) and (2,3). The right lower pane shows the magnitudes (using a color scheme) of the energy coefficients for each of the components corresponding to the level 2 nodes. Thus, the bottom section corresponds to the coefficients associated with the component (2,0), the higher section to the component (2,1) and so on. It is clear from the figure that most of the energy coefficients of the signal are concentrated in the (2,0) approximation component. A plot of the coefficients in the component (2,0) is shown in the left lower pane. Observe that the grading of the horizontal axis in the pane is graded only to about 1500. This is
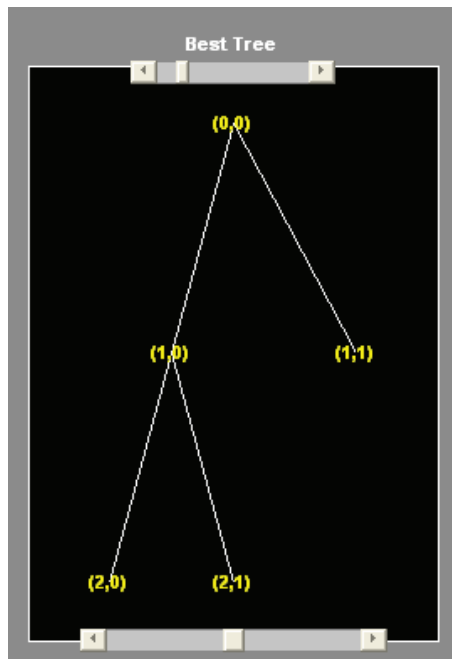
Figure 11 Best tree for the wavelet packet analysis of Figure 9

due to the fact that in computing the successive approximations using wavelets, only every other point needs to be kept. Thus, with two levels of approximation every fourth point (in this case, every fourth day) is kept. Since at each level of analysis, every component of the signal gets broken down further into approximation and detail, we have the option of not carrying out this breakdown if the either one of the resulting components possesses very small coefficients. This leads us to considering best trees for a signal. The result of finding the best tree for our temperature record is shown in Figure 11 In this case the best tree coincides with the usual wavelet tree. This also confirms the finding that the approximation (2,0) contains the significant part of the signal. From a different viewpoint, we could ask: what happens if, in the wavelet packet tree we discard all the insignificant coefficients, i.e., set them equal to zero. This is the idea of wavelet packet compression, which is one of the huge success stories of wavelet transforms. One way to do this compression is to set to zero all coefficients that are less than a pre-assigned threshold. Figure 12 clarifies the compression of the temperature record at Arar. Referring to the upper left pane in Figure 12, the vertical dashed yellow line represents the preset threshold (a little more than 8), so we are requesting that all coefficients less than 8 be set to zero. The intersection of the threshold line with the upper pink line gives the percentage of the energy of the original signal which would be retained for the chosen threshold. The intersection of the threshold line with the lower blue line gives the percentage of the coefficients which would be set to zero for chosen threshold. In this case, by choosing a threshold of 8 we retain 99.7% of the total energy of the signal while setting about 75% of the energy coefficients to zero. In other words, we can save 75% of the storage space and retain 99.7% of the total energy of the
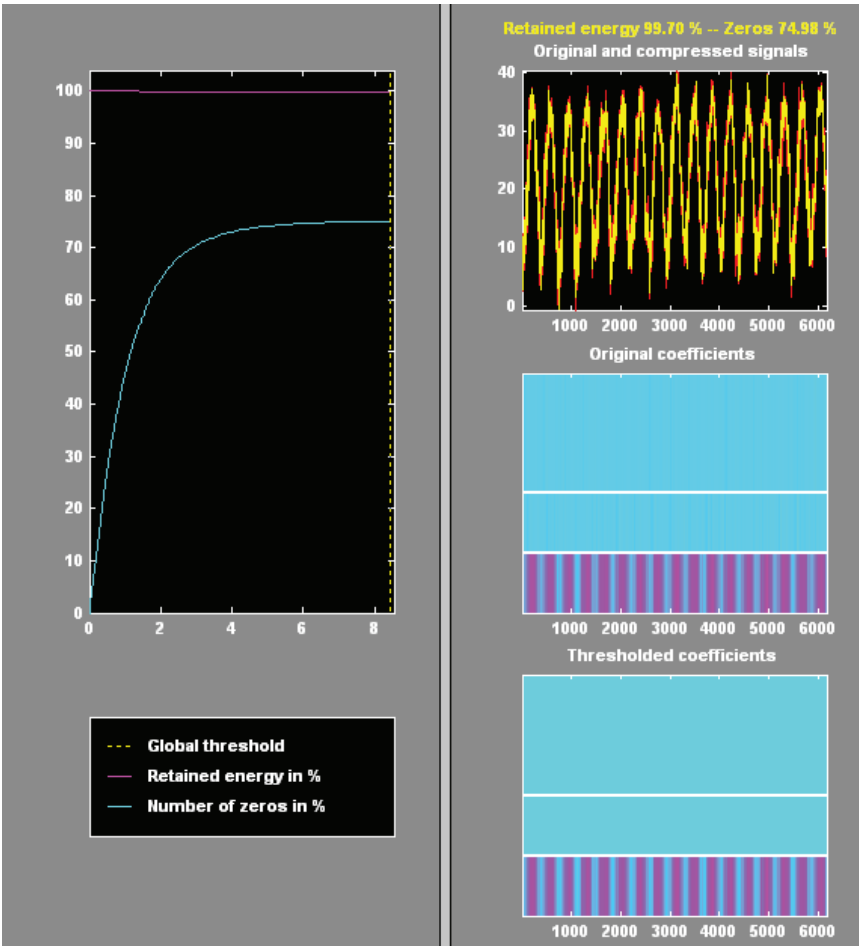
Figure 12 Compressed temperature records with the DB3 packet

signal in the remaining 25% of the coefficients. Incidentally, these are precisely the coefficients of the component (2,0) of the signal which we discussed earlier. The upper right pane shows the reconstructed compressed signal plotted in yellow on top of the original signal for comparison purposes.

WAVELET ANALYSIS OF DAILY TOTAL RAINFALL RECORD

Here we carry out the wavelet analysis of the rainfall record from Arar in the same way as we did with the temperature record. The continuous wavelet transform with the Haar wavelet of the rainfall total (RFT) record is shown in Figure 13. As most of Saudi Arabia is barren land with very little rainfall, we see in the scalogram that most of the rainfall values are near zero (the color is close to the minimum color in most of the graph area). The coefficient line drawn at the scale $a = 120$, however, reveals an interesting pattern of rain fall that repeats roughly every 3 years. Each period of 3 years appears to contain an episode of higher rainfall activity in addition to one of relatively lower
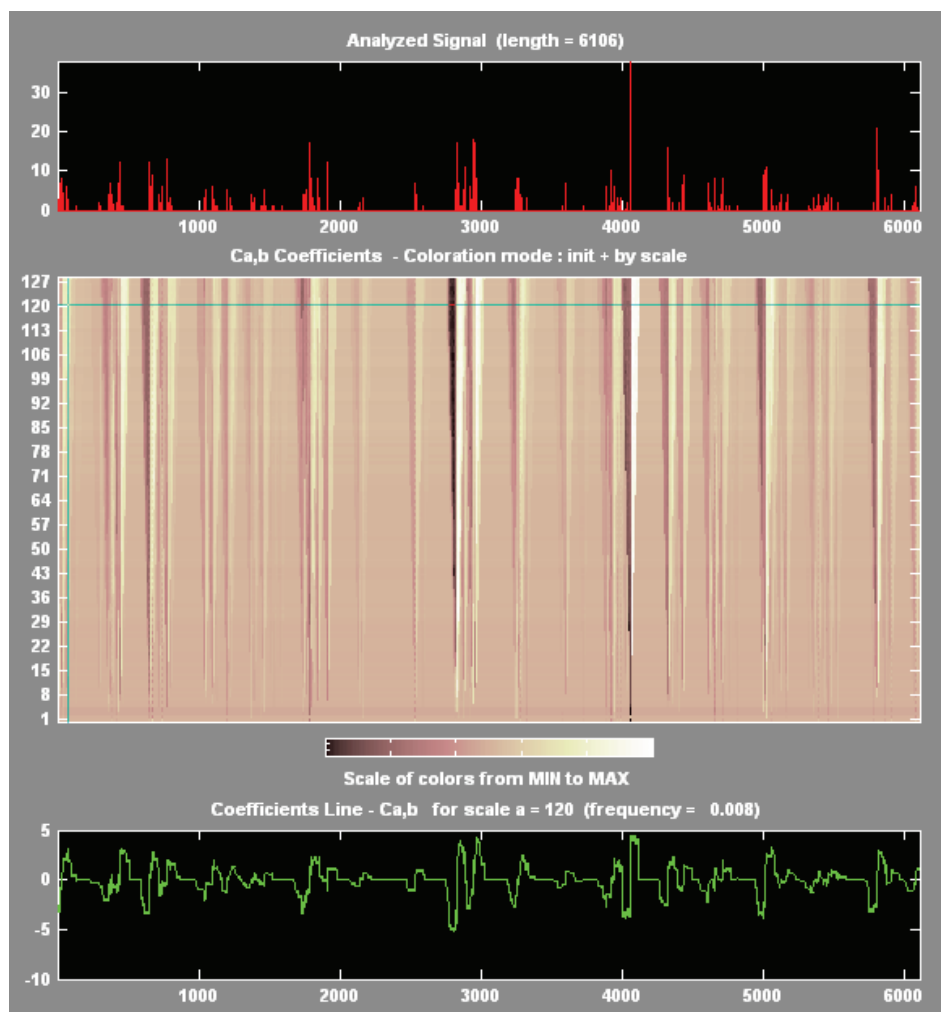
Figure 13 Continuous wavelet transform of the rainfall at ARAR

activity. The coefficient line in Figure 13 indicates that the year 1998 (around 3000 days) appears to have enjoyed exceptionally higher precipitation than the rest of the 17 year period of recording. (See the chart in Figure 1). The Haar wavelet DWT shown in Figure 14, however, reveals more. At 11 levels of resolution, the approximation level a_{11} has a decreasing trend over the past 16 year period. The trend falls from an average RFT of 0.15mm/day to 0.11mm/day. This means that there is a desertification trend at least in the area of Arar. The periodic activity observed in the CWT is also visible in the details d_8 and d_9. We should point out here that, due to the sparseness of the data and its irregularity, the Haar wavelet is expected to do a better job analyzing it. This is because we do not expect any smooth components of the signal under the circumstances. This becomes clear as we attempt to do data compression using the Haar wavelet packet and compare with what happens when we do the same with a Meyer
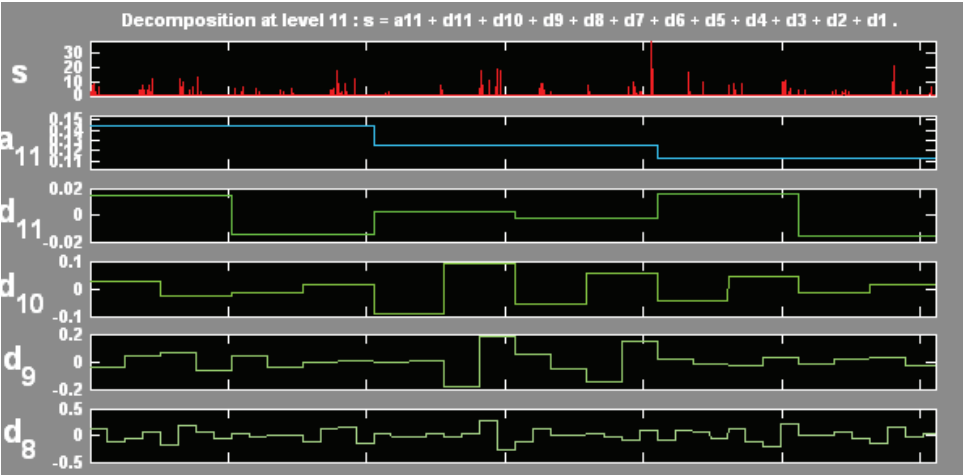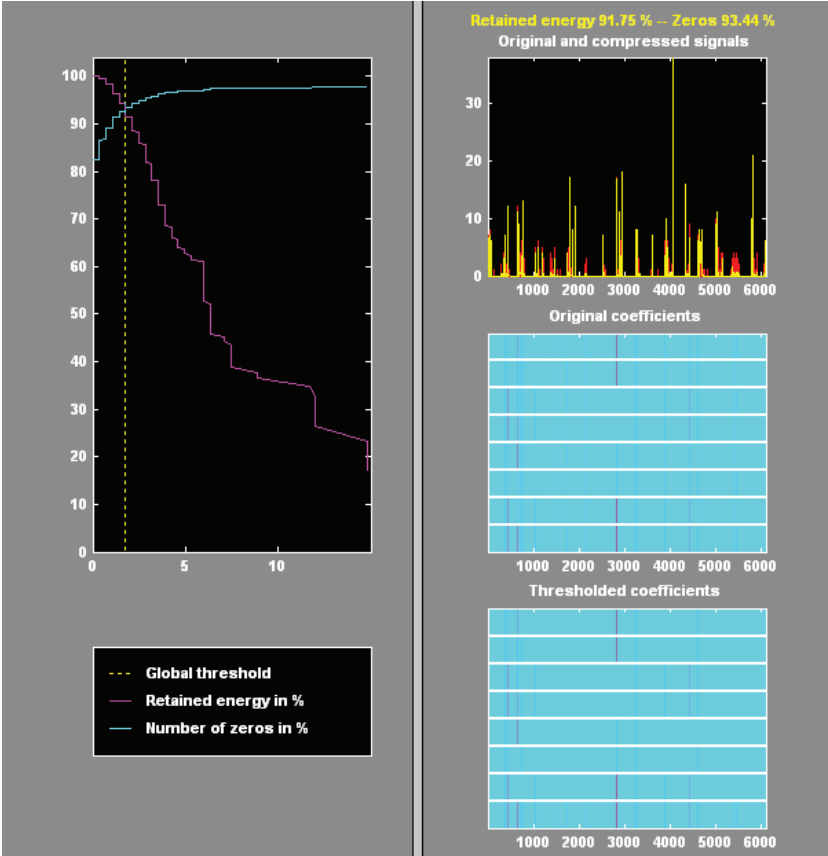
Figure 14 DWT of rainfall records at Arar

Figure 15 Compression of the rainfall data with Haar packet

wavelet. Figure 15 shows that we can retain set 93% of the coefficients to zero and still retain 91% of the energy. Compression with the Meyer wavelet (not shown here) resulted in retaining only 82% of the energy while setting 78% of the coefficients to zero. The discrepancy is undoubtedly attributed to the fact that the smooth part of the signal is simply nonexistent.

ANALYSIS OF THE RELATIVE HUMIDITY RECORD

Figure 16 shows the DWT of the relative humidity at Arar with the Meyer wavelet which was chosen because of the apparent periodic structure of the raw data. The smooth approximation level a_{12} seems to indicate that there is a long term periodic behavior of about 34 years. Our conjecture is that what we are seeing here is half a period of this long term trend. It should be interesting to observe this long term trend in the coming years. The details d_{11} and d_{12} do not modify this behavior much because of the relative amplitudes of the details in comparison with the approximation. The valley of this long term trend line coincides with the highest precipitation observed in Arar during the year of 1998. The detail d_9 shows a one time peak of high humidity around the year 1997. This peak was also observed in the CWT transform of the data (not shown here). The detail d_8 reveals the usual seasonal periodic behavior of the relative humidity. The weather is most humid during the autumn season of every year and least humid during the spring season. Figure 17 shows the Meyer wavelet packet transform of the RH data. We configured the display to show the energy content of each tree node and to show the compressed signal in the lower left pane. The compression performed in this case retains 98% of the energy while setting 87% of the coefficients to zero. This means

that we retain only 13% of the coefficients of the original signal.

ANALYSIS OF BAROMETRIC PRESSURE RECORDS

The Mayer wavelet DWT of the barometric pressure records is shown in Figure 18. The reader will notice that the decomposed signal exhibits the same general structure as that of the relative humidity and to some extent as that of the temperature. Again, the approximation component a_{12} of the signal appears to have a long term periodic behavior as was the case with the relative humidity, but with a longer period. It appears that the signal needs about two more years to come back to the same level, so we estimate the long term period to be about 38 years. The valley of this long term pressure line coincides with the lowest relative humidity and highest precipitation of the last two sections. The regular seasonal variations are exhibited by the detail d_8. The compression with the Meyer wavelet packet showed that 100% of the energy of the signal can be retained while setting 84.7% of the coefficients to zero. Of course this is attributed to the fact that the atmospheric pressure itself does not vary much about its mean value, so all we need to keep is a subsample of the approximation coefficients.

ANALYSIS OF THE WIND SPEED RECORD

The Meyer wavelet DWT of the wind speed record is shown in Figure 19. The approximation level a_{12} appears to exhibit long term periodicity of about 34 years as was the case with relative humidity and barometric pressure. The seasonal variations of the wind speed as depicted by the detail d_8 show a less regular pattern of wind speed variation.
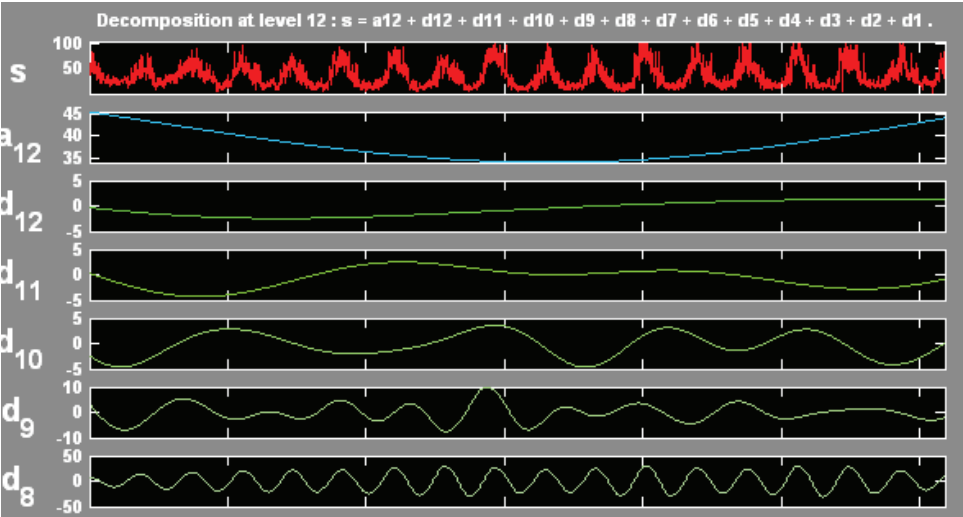
Figure 16 Meyer wavelet transform of relative humidity records
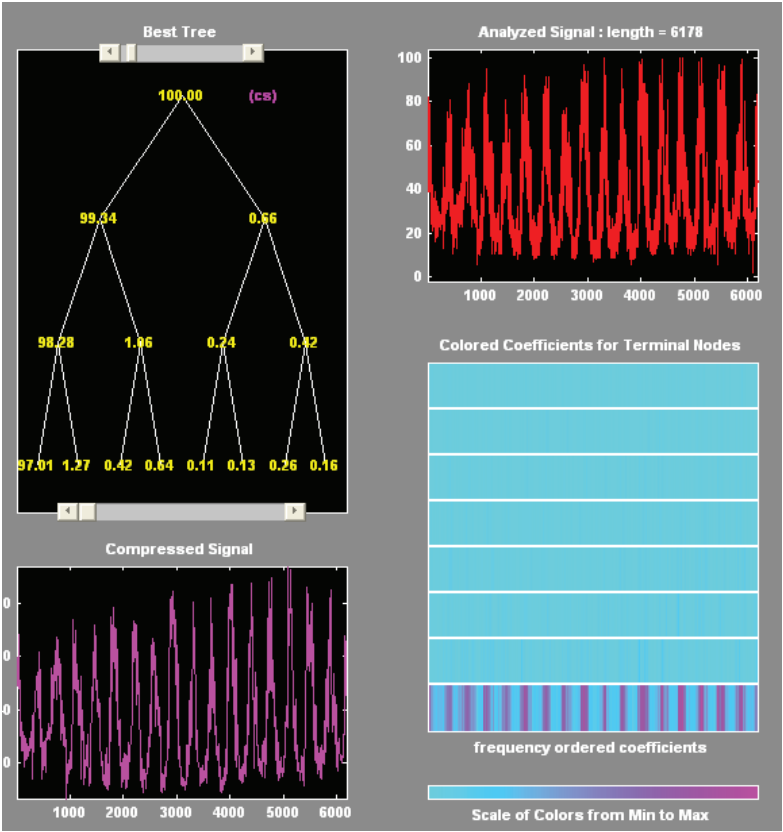

Figure 17 Meyer wavelet packet transforms of the relative humidity records
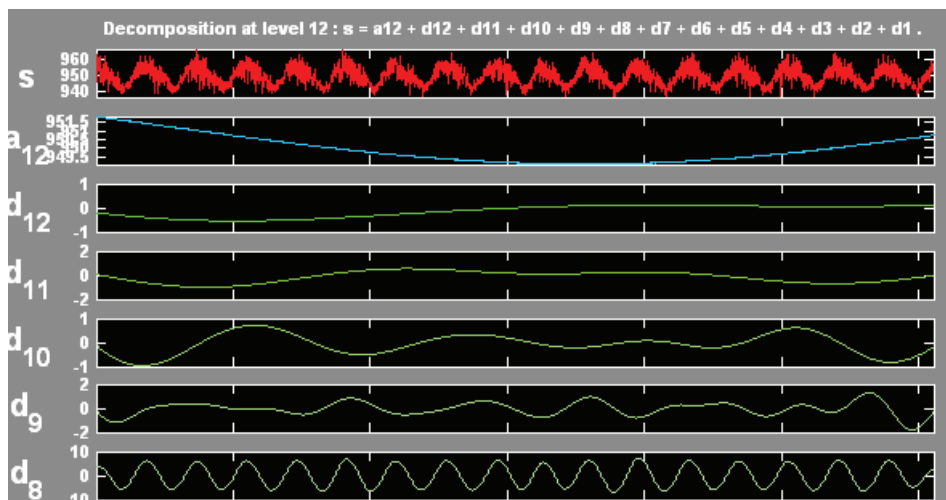
Figure 18 Meyer wavelet DWT of the barometric pressure records at Arar
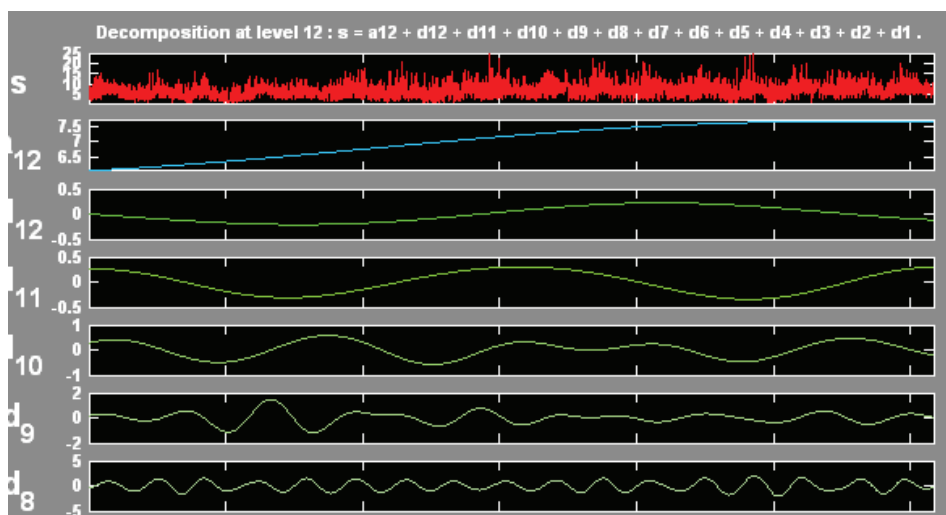

Figure 19 Meyer wavelet DWT of wind speed records at Arar

The detail level d_9 indicates a spike in wind speeds during 1993. Figure 20 shows the coefficients of the terminal nodes for both the Meyer wavelet packet (left) and Meyer wavelet DWT (right). The color code in this figure is the same as the one depicted in Figure 10. What is striking about these two figures is that they display large magnitude coefficients (pink color) for all components of the decomposition. This is the whole mark of a fractal structure of the signal which should be further investigated. As it may be expected, since all frequency ranges contribute significantly to the total energy of the signal, the compression of the wind speed signal does not achieve as impressive ratios as the other records analyzed above. For example, in order to retain 97% of the original energy, only 69% of the coefficients can be set to zero.
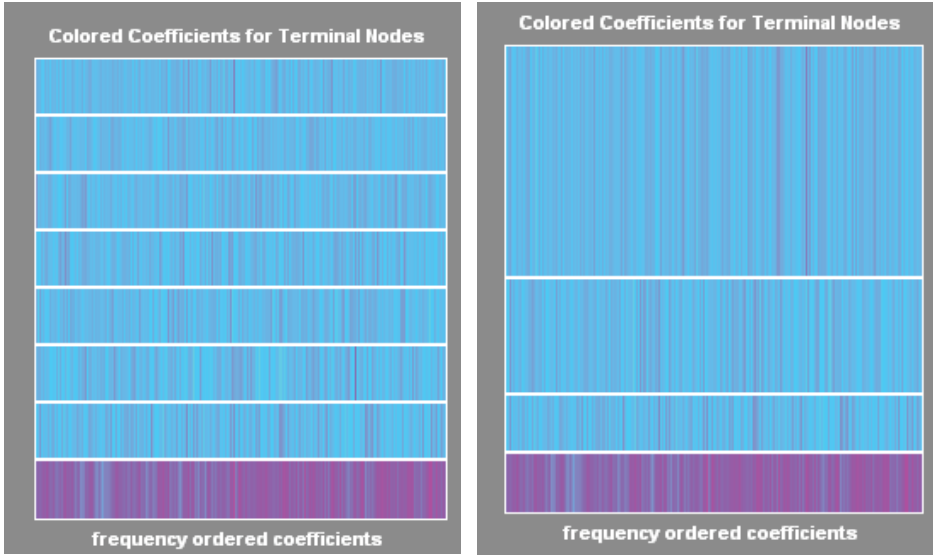
Figure 20 Coefficients of the terminal nodes for the wavelet packet (left) and the wavelet tree (right)

CONCLUDING REMARKS

The wavelet analysis of meteorological parameters can be summarized as follows:

- The CWT analysis of the temperature time series indicated that there are lesser fluctuations during the summer than the winter time in daily mean temperatures. The monthly fluctuations were also indicated by the presence of higher harmonic fluctuations.

- The DWT analysis of the temperature time series performed using the Haar and Meyer wavelets showed a general trend of heating of the local air i.e. an increase of about 1.5% per year. As a result of the smoothness of the Meyer wavelet, the shape of the approximation, or trend, signal (a_8) is not obscured by the wavelet shape and one can see a sharp average temperature change that occurred around 1991 at the time of the gulf war. This rapid change in temperature was also evident from the behavior of the higher frequency components d_9 and d_{10} around 1991.

- The wavelet packet compression of the temperature time series performed using the Daubichi wavelet packet db3 with depth of analysis 2 resulted in retention of 99.7% of the total energy of the signal while setting about 75% of the energy coefficients to zero. In other words, one can save 75% of the storage space and retain 99.7% of the total energy of the signal in the remaining 25% of the coefficients.

- The CWT analysis of rainfall data with the Haar wavelet revealed an interesting pattern of rainfall that repeats roughly every 3 years. Each period of 3 years appears to contain an episode of higher rainfall activity in addition to one of a relatively lower activity. The year 1998 received exceptionally higher precipitation.

- The Haar wavelet DWT analysis indicated a decreasing trend over the past 16 year period in the rainfall. The trend

showed a decrease from an average RFT of 0.15mm/day to 0.11mm/day. This means that there is a desertification trend at least in the area of Arar.

- The compression with the Meyer wavelet packet resulted in retaining 27% of the data with 82% of the energy.

- The DWT analysis of the daily mean values of the relative humidity at detail d_8 revealed a usual seasonal periodic behavior of the property. The weather was found to be most humid during the autumn season of every year and least during the spring season.

- There appears to be a long term period of relative humidity activity of 34 years.

- The compression performed retained 98% of the energy by setting 87% of the coefficients to zero. This means that one can retain only 13% of the coefficients without losing the original signal.

- The Mayer wavelet DWT of the barometric pressure records appears to indicate a long term trend of periodic behavior of period 38 years. The period of lowest barometric pressure coincides with that of lowest relative humidity. The regular seasonal variations are exhibited by the details at level d_8.

- The compression with the Meyer wavelet packet showed that 100% of the energy of the signal can be retained while setting 84.7% of the coefficients to zero. This is because the fluctuations of the signal around its mean value are mostly insignificant.

- The Meyer wavelet DWT of the wind speed records appears to exhibit a long term periodic behavior of period 34 years. The seasonal variations of the wind speed as depicted by the detail d_8 exhibit a less regular pattern.

- The compression of the wind speed signal could not achieve impressive ratios as in the case of the other parameters analyzed above. In order to retain 97% of the original energy, only 69% of the coefficients can be set to zero. This means that all fluctuation levels about the mean contain significant information about the signal.

ACKNOWLEDGEMENT

BIOGRAPHICAL NOTES

Dr. Mohamed El-Gebeily is a full professor in the Department of Mathematics and Statistics since 2004. He received his PhD degree from Oklahoma State University, USA in 1984 in Mathematics and his BS degree from Alexandria University, Egypt in 1975 in Electrical Engineering. He is interested in applications of functional analysis in areas such as wavelet applications and differential equations.

Shafiqur Rehman is a Research Engineer at Center for Engineering Research in Research Institute of King Fahd University of Petroleum and Minerals (KFUPM). He has more than twenty years of research experience in surface and upper air meteorology, wind and solar energy assessment, wind/pv/diesel hybrid power system design with and without battery

backup, meteorological data measurements using 40 to 60 meter tall towers, and recently has developed interest in geothermal power resources assessment and global warming issues and trending. He has published and presented more than 100 research papers in international refereed journals and conferences. He has been invited as key note speaker in various international conferences and presented more than 20 papers in different conferences. He has chaired and co-chaired technical sessions at international conferences and congress. He has been awarded Distinguished Researchers Award in 2007 by KFUPM. He is refereeing research papers for around 20 journals related to his field of interest.

Dr. Luai M. Al-Hadhrami is assistant professor of thermo-fluid at King Fahd University of Petroleum and Minerals (KFUPM), Dhahran, Saudi Arabia. He received his Ph.D. in 2002 from Texas A&M University-college Station. His research interests are gas turbine, energy systems, failure analysis. He has published 22 articles in well-recognized journals, and conference proceedings. He is the center director for engineering research-Research Institute at KFUPM.

Dr. Jaafar AlMutawa received B. Sc. and M. Sc. degrees in Mathematics from University of Bahrain in 1994 and 1999, respectively, and the Ph.D. degree from Kyoto University in 2006. He has been a member of the Department of Mathematics and Statistics, since 2006. He had a visiting researcher position at Kyoto University from July 2007 to September 2007. His research interests include system identification, estimation theory, stochastic realization, subspace method of identification, blind identification, and control of industrial processes.

REFERENCES

Alkolibi, F. 2002. Possible effects of global warming on agriculture and water resources in Saudi Arabia: impacts and responses. *Climatic Change* **54**: 225–245

Baliunas, S., Frick P., Sokoloff D. & Soon W. 1997. Time scales and trends in central England temperature data (1659–1990): a wavelet analysis. *Geophysical Research Letters* **24**: 1351–1354

Dabuechies, I. 1990. The wavelet transforms time-frequency localization and signal analysis. IEEE Transactions on information theory 36, 5

Datsenko, N M., Shabalova M V., Sonechkin D M. 2001. Seasonality of multi-decadal and centennial variability in European temperatures: the wavelet approach. *Journal of Geophysical Research* **116**: 449–463

Ding, X., Zheng D. and Yang S. 2002. Variations of the surface temperature in Hong Kong during the last century, Int. J. Climatol. **22**:715–730

Elagib, N A. and Addin Abdu A S. 1997. Climate variability and aridity in Bahrain. *Journal of Arid Environment* **36**:405-419.

Freiwana, M. and Kadioglub M. 2008. Climate variability in Jordan. *Int. J. Climatol.* **28**: 69–89 (2008)

IPCC 2001. Climate Change 2001. Synthesis Report, Cambridge University Press, Cambridge, UK, 2001, 397 pp

Lau, K M. and Weng, H. 1995. Climate signal detection using wavelet transform: how to make a time series sing. *Bulletin of the American Meteorological Society* **76**: 2391–2406

Malat, S. 1998. A wavelet tour of signal processing, Academic Press, New York, NY

Meehl, G A., Washington, W M., Ammann, C M., Arblaster, J M., Wigley T M L. and Tebaldi, C. 2004. Combinations of natural and anthropogenic forcings in twentieth-century climate. *J. Climate*. **17**:3721–3727.

Nicholls, N. and Collins, D. 2006. Observed Climate Change in Australia Over the Past Century. *Energy & Environment* **17(1)**:1-12

Park, J., Mann, M E. 2000. Interannual temperature events and shifts in global temperature: a multiple wavelet correlation approach. *Earth Interactions* **4**: 1–53

Partal, T., Kucuk, M. 2006. Long-term trend analysis using discrete wavelet components of annual precipitations measurements in Marmara region (Turkey). Physics and Chemistry of the Earth 31, 1189–1200

Percival, D B. and Walden A T. 2000. Wavelet Methods for Time Series Analysis. Cabridge University Press: Cambridge.

Pisoft, P., Kalvova, J. & Brazdil, R. 2004. Cycles and trends in the Czech temperature series using wavelet transforms. Int. J. Climatology 24:1661-1670

Rehman, S., El-Gebeily, M. Long-Term Behavior of Meteorological Parameters In Saudi Arabia *Submitted*

Sonechkin, D M., Astafyeva N M., Datsenko, N M., Ivachtchenko, N N. & Jakubiak, B.1999. Multiscale oscillations of the global climate system as revealed by wavelet transform of observational data time series. *Theoretical and Applied Climatology* **64**: 131–142

Walnut, D. 2002. An Introduction to Wavelet Analysis Birkhäuser Boston.

Yueqing, X., Shuangcheng, L. and Yunlong, C. 2004. Wavelet analysis of rainfall variation in the Hebei Plain. Science in China series D Earth Sciences 48, 2241–2250